On the implementation of green airport facilities by integrating electric airplanes: A case study

A potential solution for future green airports

Oscar Larsson

Faculty of Health, Science and Technology
Electrical Engineering Department
Bachelor Thesis: 22.5HP
Internal Supervisor: Andreas Theocharis
External Supervisor: Tomas Forsberg, Jonas Persson
Examinor: Magnus Mossberg
Date: 13 January 2023

Abstract

Following continued emission of greenhouse gases climate change is increasingly becoming a greater threat to the continued well-being of people around the world. While airports contribute around 2.5% of the global greenhouse emissions it delivers the greenhouse gases higher up in the atmosphere which increases the negative effect of greenhouse gases. In response airports around Sweden are working towards implementing green airports and flights. This will be done in part by supplying the facility with green energy from local green power facilities but also in part by replacing the traditional fuel from petroleum-based flights to electrical flights. This report examines the required solar plant to support both the existing facility and the future planned electrical flights with solar energy. This report will examine the required size and configuration of the solar plant to supply necessary power with the help of the simulation tool SAM and weather data from NSRDB. This report will also investigate the current system capabilities and required changes to handle the increased load demand and power production into the facility using power flow simulations of the current system with the future loads

Table of Contents

1. Acronyms:

Acronym	**Word**
SAM	System Advisory model
NSRDB	National Solar Radiation Database
AI	Artificial Intelligence
ESS	Energy Storage System
MPPT	Maximum power point tracker
PWM	Pulse Width Modulation
DNI	Direct Normal Irradiance
GHI	Global Horizontal Irradiance
DHI	Diffuse Horizontal Irradiance
EMI	Electro Magnetic Interference
NREL	National Renewable Energy Laboratory
LVP	Low Visibility Procedure
LFV	Luftfartsverket
IoT	Internet of Things

2. Introduction:

The airport sector accounts for around 5% of the global greenhouse gas emissions and is expected to increase in the future with flights steadily increasing from the early 2000s until 2020 with the SARS-covid pandemic decreasing the number of flights from 40.3 million in early 2020 to 16.9 million later during 2020 [1]. Global annual flights are on the increase since the sharp decrease in 2020 which is leading to the increase of greenhouse emissions from the flight sector. Reducing greenhouse emissions is crucial to reduce the effect of global climate change and decarbonizing the flight sector is a crucial step to a more sustainable industry. Decarbonisation of the energy supply chain is accomplished by introducing sustainable and environmentally friendly energy production and consumption processes. It is of primary importance to sustain the energy balance between production and demand for the stability and the security of an electrical grid. That is to maintain the frequency and the voltage levels in about the rated values aiming to avoid black-outs. Making the energy production secure and balanced is difficult when integrating solar and wind energy because their energy production is non-plannable which in turn makes the task of integrating more loads into the system more difficult [2] [3]. To avoid grid failures and unforeseen interactions due to differences between power demand and production optimized power management solutions are required for stable operability of the electricity system [4] [5] [6] [7]. Due to great advancements in AI, big data analytics and IoT energy prediction and planning could be supported using these technologies instead of using grey and white-box prediction methods when performing system performance studies [8] [9] [10] [11]. Due to individual consumers having different consumption profiles load predictions are difficult, but by IoT integration into intelligent grids power predictions could become more accurate, combining this with ESS it could have a prominent role in relieving the power grid and also used in energy exchange [12] [13].

Karlstad airport is located outside of Karlstad in Våldalen. Karlstad is an ideal city to implement solar power because of its high solar hours ranking on 9th place among the other Swedish cities. [14]. Karlstad airport is the largest airport in the region of Värmland receiving around 100 000 passengers annually. Karlstad airport have suggested implementing a solar park facility capable of supplying the entire facility with green electrical energy with the help of an ESS. Introducing electrical planes can lead to great increases in the daily loads on the airports grid system which in turn lead to increased degradation of the system because of the increased load on the system. Overloading the existing system can also lead to a complete system failure if the system is loaded heavily for a longer period of time.

2.1 Assumptions for this project:

In this project several assumptions will be made about the current system and the future systems that will be implemented. The reason for this would be that either insufficient data exists to make a fully nuanced evaluation or that it is outside the scope of a bachelor grade project. Some of the following assumptions will be made.

No snowfall over the solar park during winter: Due to that the most recent hourly snow fall data from NSDAP comes from 1986 and because of switching trends in weather due to climate change, no snow data will be included in the simulation of the solar plant.

For any system the three phases will be equally loaded: Because of insufficient data over the loads of each of the phases, a detailed calculation and analysis of the load on each phase is not possible. In this project, all loads will be treated as a balanced three phase system with no phase shifting occurring on any of them.

2.2 Purpose:

The purpose of this study project is to investigate some possible way to implement a green airport completely powered by solar power supported by an ESS. To do this, the project will look at the following:

- Design a solar plant capable of covering the annual energy consumption of Karlstad airport and investigate its impacts on the current grid system.
- Investigate the status of the existing grid system by analysing the systems current loads, load trends and grid structure to evaluate the systems current performance.
- Investigate the broad impacts of inserting plane chargers into the current system and what consequences might be present from inserting the added loads into the systems.

- Using previously investigated information to construct a suggested implementation for the future system.

3. Theory:

3.1 Solar Geometry and Irradiance:

Solar declination is the tilt of the polar line relative to the perpendicular line from the sun. This declination can be estimated by the following equation:

$$\delta = \left(\frac{180}{\pi}\right) * (0.006918 - 0.399912 * \cos(B) + 0.070257 * \sin(B) - 0.006758 * \cos(2B) + 0.000907 * \sin(2B) - 0.002697 * \cos(3B) + 0.00148 * \sin(3B)) \quad (1)$$

Where B is described by:

$$B = (n-1) * \left(\frac{360}{365}\right)$$

Where n is the nth day of the year.

The angle of the

$$\varphi_{ssr} = \operatorname{acos}(-\tan(\phi) * \tan(\delta)) \quad (2)$$

Where δ is the solar declination and ϕ is the latitude of the location φ_{ssr} is the angle where sunrise and sunset occur.

The hour angle is the angle to the sun relative to the local meridian that the location is. Because the earth rotates once per day, the hour angle can be described by the equation:

$$\varphi = 15 * (12 - h) \quad (3)$$

Where h is the hour of the day.

There are several models for estimating the total solar irradiance that falls on a tilted surface. Some of the more widely used models are the isotropic model, the HDKR model and the Perez model. The first two models, the isotropic and HDKR model are simpler to implement and can be used with the information provided about the sites for evaluating the expected power production. In this project the focus will be on the HDKR model because it provides more accurate simulations while still being easier to implement into code.

The HDKR model consists of the following equation:

$$\lambda_T = (\lambda_b + \lambda_d * A_i) * R_b + \lambda_d * (1 - A_i)\left(\frac{1 + cos\beta}{2}\right) * \left(1 + f * \sin^3\left(\frac{\beta}{2}\right)\right) + \lambda * P_g * \left(\frac{1 - cos\beta}{2}\right) \quad (4)$$

Where λ_T is the total solar irradiance per hour [J/mm^2 *h], λ_b is the beam irradiance also referred to as DNI per hour [J/mm^2 *h], λ_d is the diffuse horizontal irradiance also referred to as DHI. β is the tilt angle of the surface, λ is the total solar irradiance that falls on a surface horizontal to the ground per hour which also is referred to as GHI [J/mm^2 *h], I_0 is the total extra terrestrial irradiance that falls on a horizontal surface every hour [J/mm^2 *h] and it can be estimated using the following equation:

$$\lambda_0 = G_{sc} * (1 + 0.033 * \cos\left(360 * \frac{n}{365}\right) * (cos\phi * \cos\delta * \cos\varphi + \sin\phi * \sin\delta) \quad (5)$$

Where G_{sc} is the solar constant [W/mm^2], n is the nth day of the year, ϕ is the latitude of the surface, δ is the solar declination and φ is the hour angle

P_g is the diffuse reflectance of the surroundings which also is referred to as albedo. f is a modulating factor to correct for cloudiness which is describes by the equation:

$$f = \sqrt{(\frac{\lambda_b}{\lambda})} \tag{6}$$

R_b is the geometric factor which when the surface is situated in the northern hemisphere can be described by the equation:

$$R_b = \frac{\cos(\Phi + \beta) * cos\delta * cos\varphi + \sin(\Phi - \beta) * sin\delta}{cos\Phi * cos\delta * cos\varphi + sin\Phi * sin\delta} \tag{7}$$

A_i is the anisotropy index and is defined as the equation: [15]

$$A_i = \frac{\lambda_b}{\lambda_0} \tag{8}$$

3.2 Total solar module area to cover annual energy consumption:

If a facility would be required to be supplied by a solar power facility the annual energy requirement of the facility would need to be matched with the annual power production of the solar power facility. This can be expressed as:

$$E_{An} = E_{PVAn} \tag{9}$$

Where E_{An} is the annual energy consumption of the facility expressed in kWh and E_{PVAn} is the annual power production of the solar power facility expressed in kWh. E_{PVAn} can be expressed as the following:

$$E_{PVAn} = G_{An} * A_{PV} * \eta_t \tag{10}$$

Where G_{An} is the annual solar irradiance that falls on the surface expressed as kWh/m^2, A_{PV} is the solar panel area expressed in m^2 and η_t is the efficiency of the system which is unitless. η_t Is expressed as:

$$\eta_t = \eta_{PV} * \eta_{Inv} * \eta_{MPPT} \tag{11}$$

Where η_{PV} is the efficiency of the solar module, $\eta_{Inv}$is the efficiency of the power inverter and $\eta_{MPPT}$is the efficiency of the maximum power point tracker (MPPT).

using equation (10 in equation (9 the following equation can be derived:

$$E_{An} = G_{An} * A_{PV} * \eta_t \tag{12}$$

using equation 11 into equation 12 the following expression can be made:

$$E_{An} = G_{An} * A_{PV} * \eta_{PV} * \eta_{Inv} * \eta_{MPPT} \tag{13}$$

Replacing A_{PV} with A_{MReq} the following equation can be given:

$$E_{An} = G_{An} * A_{MReq} * \eta_{PV} * \eta_{Inv} * \eta_{MPPT} \tag{14}$$

Where A_{MReq} is the required solar module area to cover the facilities annual power consumption. With this A_{MReq} can be expressed as the following:

$$A_{MReq} = \frac{E_{An}}{G_{An} * \eta_{PV} * \eta_{Inv} * \eta_{MPPT}} \tag{15}$$

This equation can be used to estimate the required module area to cover the facility with an annual energy consumption using the parameters specified in the equation.

3.3 Evaluating the total required area of the solar plant:

A crucial design aspect of a solar power plant is the Ground coverage ratio (GCR). The ground coverage ratio can be expressed as the following equation:

$$GCR = \frac{H_{PV}}{L_{spacing}} \tag{16}$$

Where $L_{spacing}$ is the space length between each row of arrays of solar panels and H_{PV} is the height of the solar panel. The GCR can have a value ranging from 0 < GCR < 1.

The total modular area of the solar park can be expressed as:

$$A_M = (n_b * L_b) * (L_h * n_h) * n_{row} * n_{string} \tag{17}$$

And the total area for the entire facility can be expressed as:

$$A_{tot} = (n_b * L_b) * (L_h * n_h * GCR) * n_{row} * n_{string} = A_M * GCR \tag{18}$$

Where A_{tot} is the total required area for the entire solar facility, L_b is the Length of a single solar cell, n_b is the number of solar cells per solar panel, L_h is the height of a single solar cell, n_h is the number of solar cells per solar panel, n_{row} is the number of rows of solar panel and n_{string} is the amount of strings of solar panels.

Which means that the total area required can be expressed as:

$$A_M * GCR = A_{tot} \tag{19}$$

3.4 Electrical energy consumed over a time period:

When presented with a graph like the following:

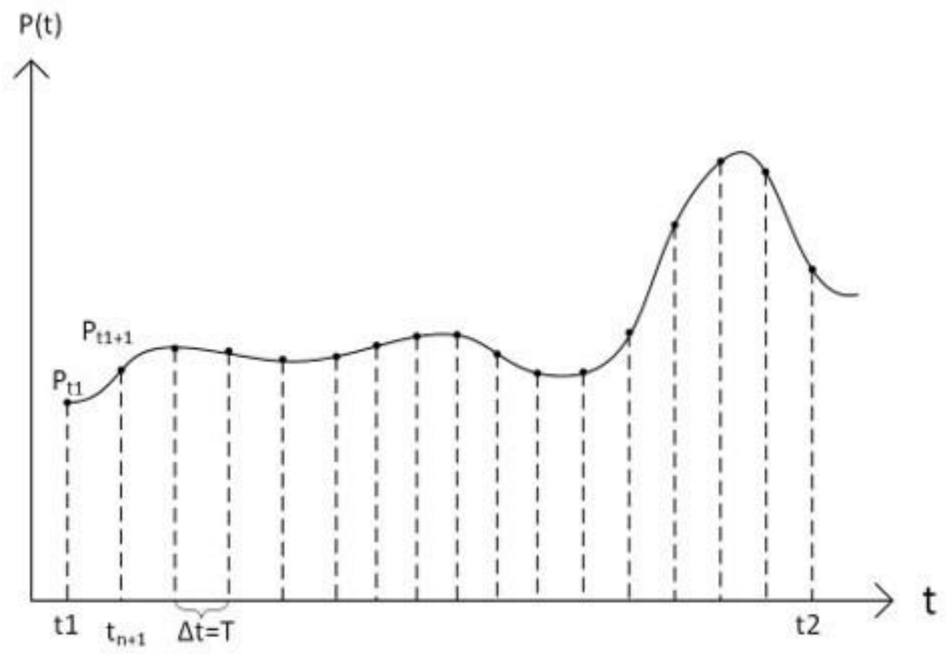

Figure 1: A continuous power graph

Where P(t) is the instantaneous power over the load expressed in Joules per second and t is the time expressed in seconds the total energy consumption of the load between t2 and t1 can be expressed as the following.

$$E = \int_{t2}^{t1} P(t) * dt \tag{20}$$

Where E is the total energy consumed over the period t1 to t2 expressed in joules.

This can also be expressed in discrete terms:

$$E = T * \sum_{n=n1}^{n2} \bar{P}[n] \tag{21}$$

Where T is the sampling time in seconds. $\bar{P}$ is the average power consumption over sampling interval n and is supposed constant during whole time T and E is the energy consumed over the time period n1 and n2.

In this project, the facility does not have a continuous power monitoring system but instead uses an energy monitoring system. This system monitors the total hourly energy consumption of the facility which leads to a graph like this:

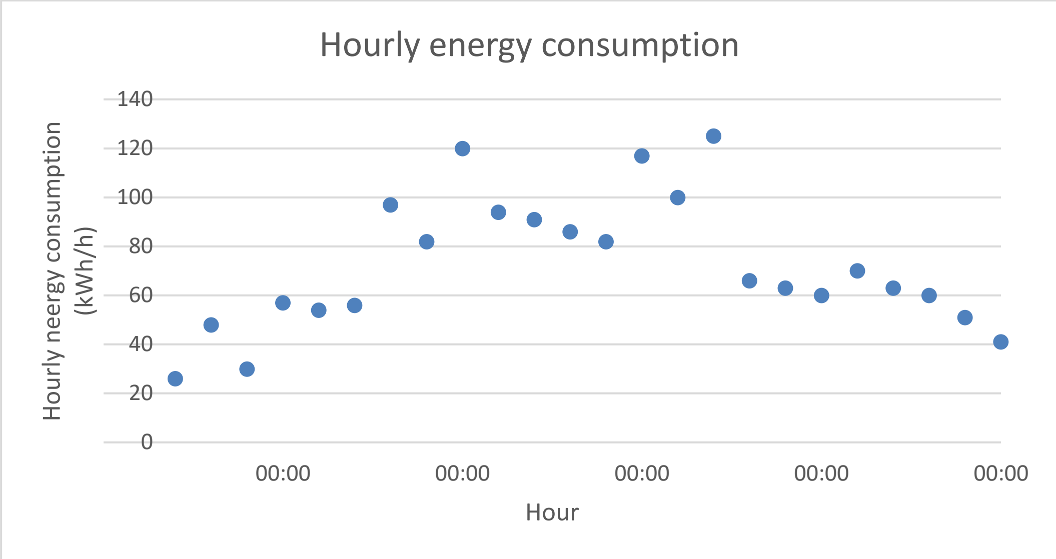

Figure 2: Hourly energy consumption graph.

Where each dot is a measuring point summarizing the total energy consumed over that particular hour. Because the energy is measured in kWh/h the alternative graph can be expressed as follows:

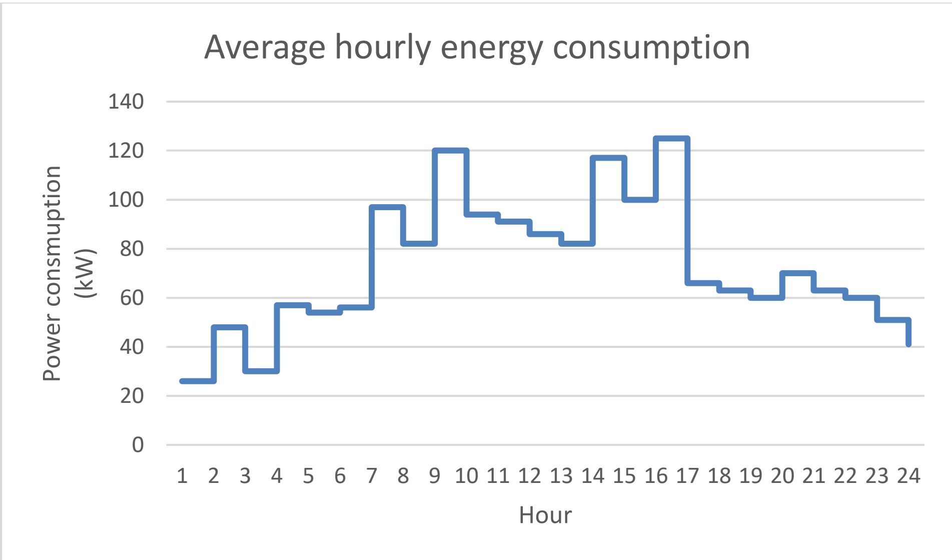

Figure 3: A power graph converted from an energy graph

This shows that the energy consumption in kWh/h can instead be expressed as an average power consumption of the facility in kW over the entire hour. Because of the limited load data over the continuous load profile of the facility this method will be used when evaluating the load profile of the facility.

The annual energy consumption E_{AN} can be determined using the following equation

$$E_{AN} = \sum_{n=1}^{24*365} \bar{P}_h\,[n] * h = \sum_{n=1}^{24*365} \bar{P}_h[n] * 1 = \sum_{n=1}^{24*365} E_h[n] \tag{22}$$

Where P_h is the average hourly power consumption expressed in [kWh/h], E_h is the hourly consumed energy of the facility expressed in [kWh], n is the nth hour of the year and E_{AN} is the annual energy consumption expressed in [kWh]

3.5 One line diagram:

A one line diagram is a method to combine the three phase system into a single line. This leads to the ability to simplify a large system into a more manageable line diagrams which allows for easier power flow analysis of the system. When analysing one line diagrams the current going through a balanced three phase system in each of the phases can be calculated with the following equation:

$$I = \frac{S_{3phase}}{\sqrt{3} * U_{3phase}} \tag{23}$$

Where the one line diagram will have aggregated loads where multiple loads on a shared transmission line will be aggregated into one larger load. This is due to the fact that the power cables between each load could have the same power rating which means that it can be viewed as a long shared cable.

The aggregation process is as follows:

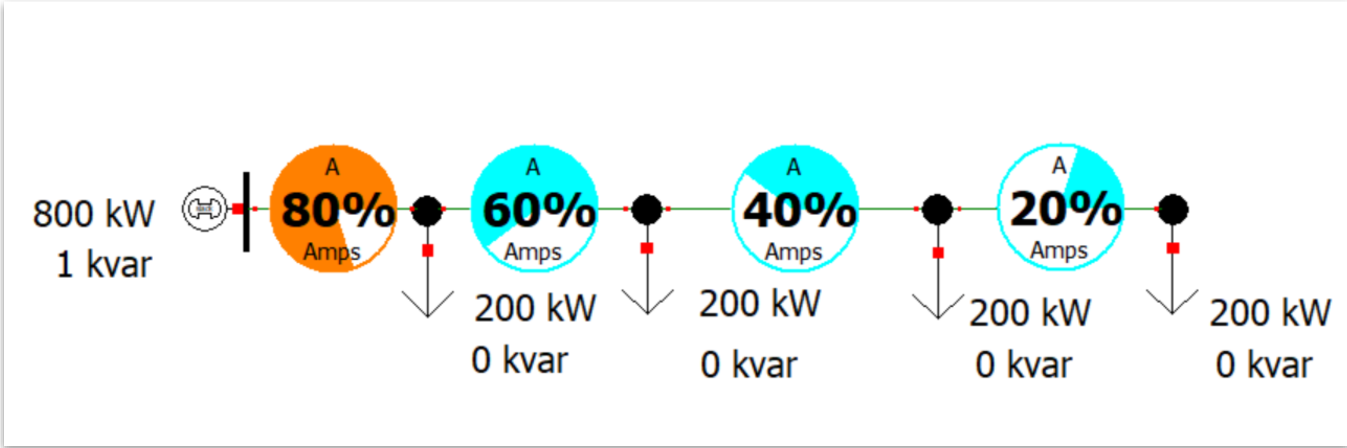

Figure 4: An example of a one line diagram

The picture above demonstrates an example load, because of this all lines connecting each of the nodes have the same rating. These four separate nodes going into separate loads can be aggregated into one larger load:

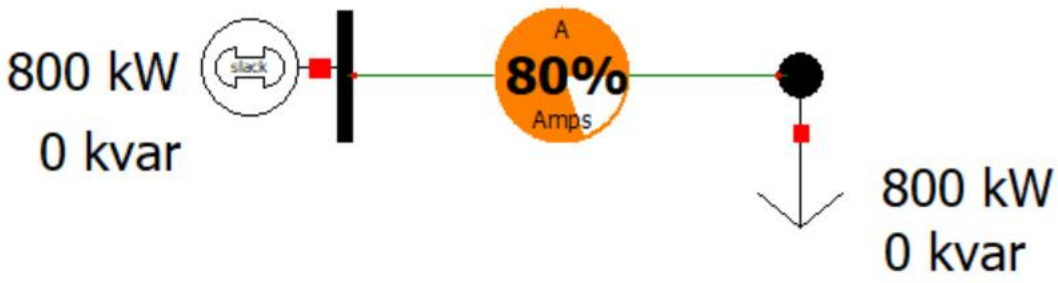

Figure 5: An aggregated one line diagram

This simplification works under the assumption that all of the phases in each load are equally loaded.

3.6 Solar cell production:

3.6.1 Simulating the optimal angle:

By using theory to predict the solar irradiance that falls on a flat surface, determining the optimal tilt angle for a fixed flat surface is possible. The resources necessary for the code to determine the optimal tilt angle is DNI, GHI, DHI, albedo and the coordinates for the location where solar panels are planned to be installed. The weather data used in this project was supplied through NSRDB for the year 2019. Figure 24 in the appendix illustrates how the code works.

4. Results and data:

4.1 Results from optimal tilt angle simulation:

After running the code, the following graph is produced:

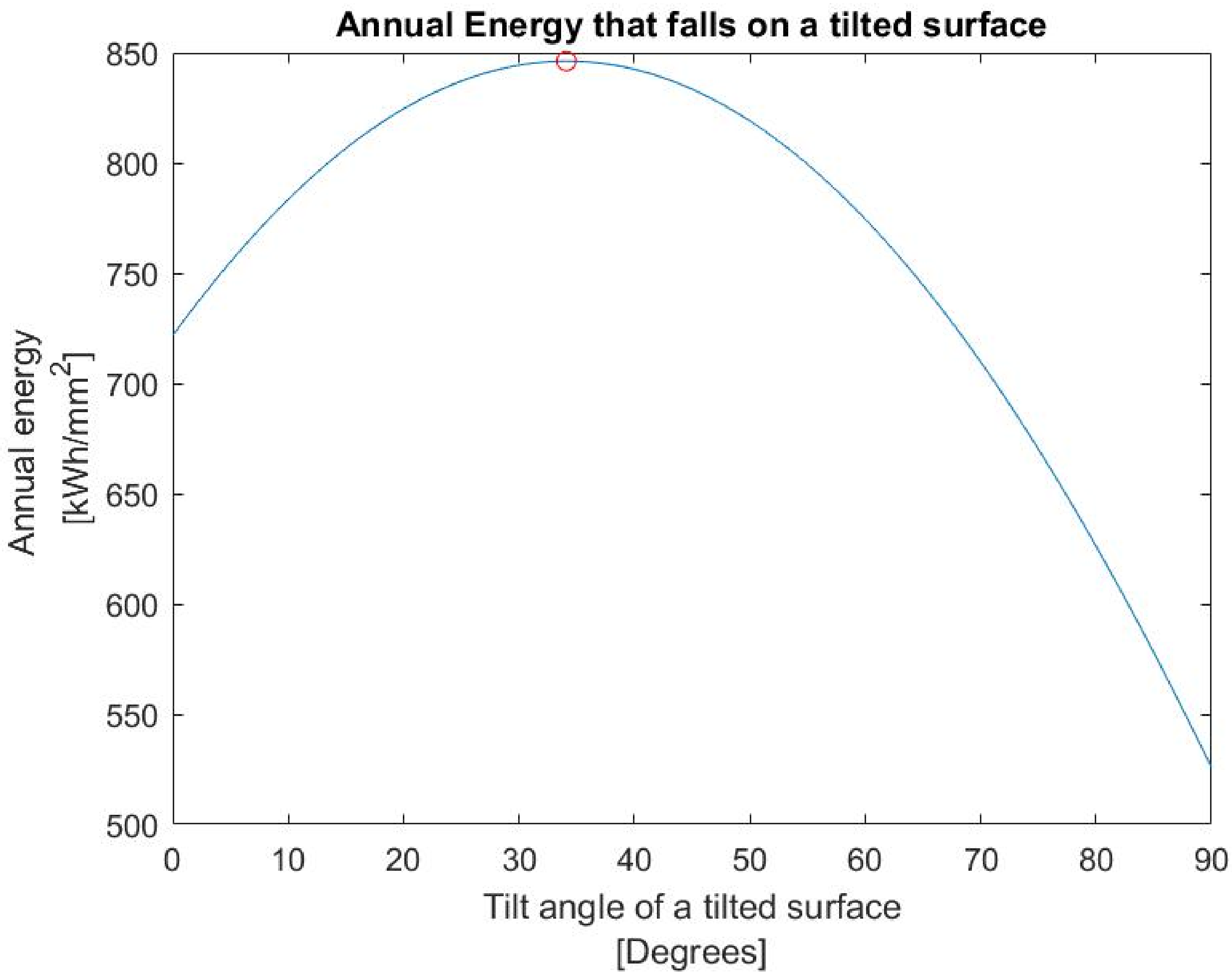

Figure 6: A curve showing the annual solar energy that falls on a surface depending on the tilt angle of the surface

As shown in Figure 6, at a tilt angle of 37.3 the annual energy that falls upon the surface is 846.173845kWh/m^2.

4.1.1 Weather data:

The weather data used in this project comes from NSRDB. The weather data is collected from multi-channeled measurements from geostationary satellites. This allows for a history of the hourly to half hourly measurements about the DNI, GHI and DHI for a particular location and time. [16]

4.2 Load profile of Karlstad airport:

At Karlstad airport the energy consumption of the facility is monitored by Ellevio for the purpose of billing the current energy consumption and additionally bill the highest hourly energy that the facility has been importing from the grid. The facility does not monitor the continuous load that the facility imports from the grid but instead collects the total energy consumption of the facility over the sampling time. The time interval between each energy sampling is once every hour and the information about the energy consumption during the sampled interval is transmitted directly to Ellevio where the information is logged to Ellevio´s website. It is from this website that the following energy load profile data has been extracted.

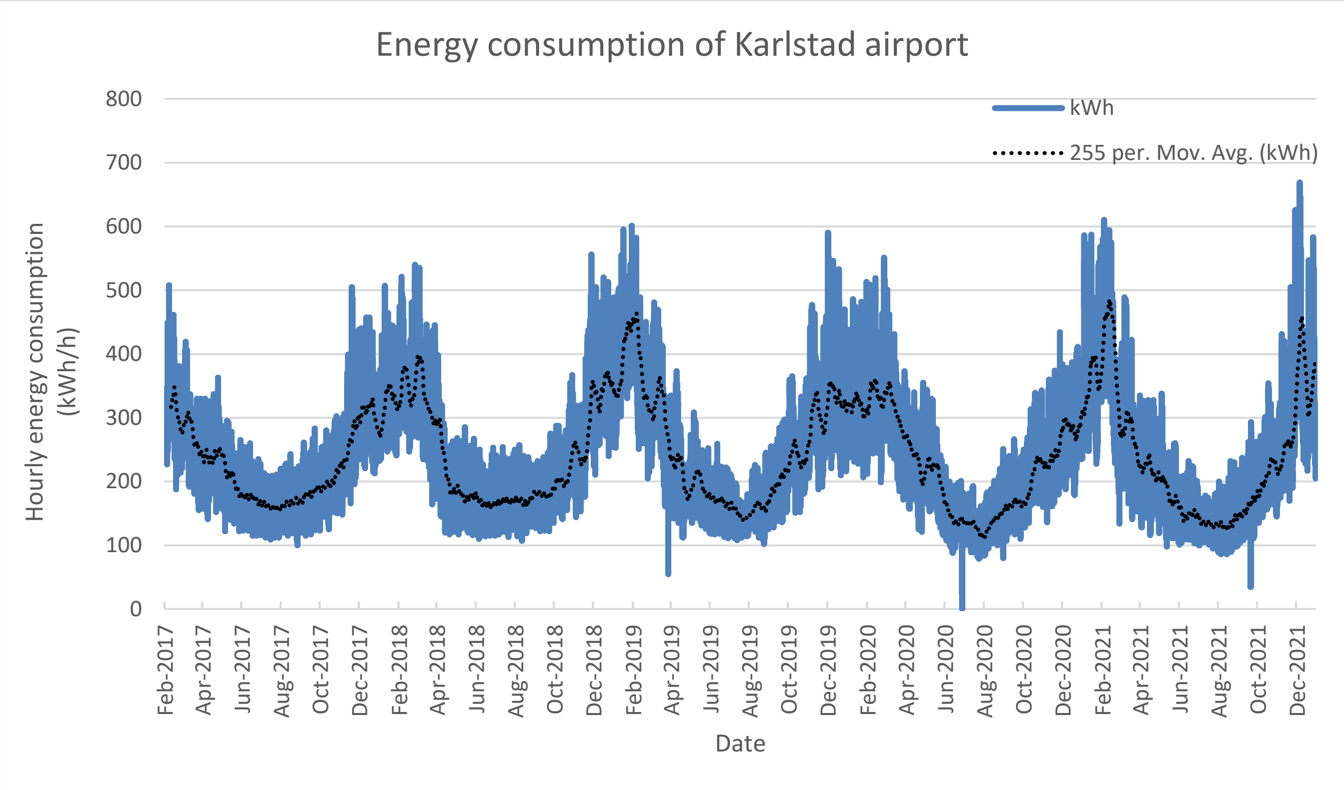

Figure 7: Hourly energy consumption from Karlstad airport from Feb-2017 to Dec-2021

Because the energy consumption of the facility is readily available this project will use this information as a guide to the specifications of the future solar plant. Mainly this will look at the annual energy requirements of the facility. Looking closer at Figure 7, the most energy intense periods are during the colder periods of the year. Since the most energy intense periods also have the highest average power consumption using these periods when evaluating the stress on the existing grid would be the most appropriate, these energy intense periods occur between November and February.

Using the load profile provided by Karlstad airport prior to any added chargers the following values are given for each of the years.

Year	Peak hourly energy load [kVAh/h]	Annual energy consumption [MWh]
2017	534,7457	1795,578
2018	569,8781	2132,397
2019	617,4957	2214,072
2020	558,7933	1987,000
2021	672,757	2091,767

Table 1: Yearly energy consumption.

4.2.1 Estimated energy load after the addition of chargers:

The addition of EV chargers will increase the load that exists on the facility's current grid network. The chargers that are investigated in this project are chargers for Heart Aerospace´s ES-19 electrical plane. These chargers are marketed for a rated charge power of 1MW and claim to be able to charge the ES-19 in 40 minutes for an average mission. It is unclear whether there are different charging levels on the chargers that could potentially decrease the power level which would lengthen the charging period but decrease the load on the system. Estimating the number of chargers will mainly depend on the specifications of the chargers, the flight schedule and the time required to charge an individual plane.

Using the daily flight schedule provided from Karlstad airport:

	Monday – Saturday	
Route	Departure	Return
Karlstad -> Oslo -> Karlstad	06:00	08:00
Karlstad -> Gothenburg -> Karlstad	06:30	08:30
Karlstad -> Oslo -> Karlstad	17:00	19:00
Karlstad -> Gothenburg -> Karlstad	17:30	19:30

Table 2: Suggested flight schedule

Because the time between each departure is around 30 minutes and the fastest possible charging time for an individual plane is 40 minutes, the airport would at least need two airplanes available to be able to meet the demand of departures.

	Monday – Saturday		
Route	Departure	Return	Plane in charge
Karlstad -> Oslo -> Karlstad	06:00	08:00	Plane 1
Karlstad -> Gothenburg -> Karlstad	06:30	08:30	Plane 2
Karlstad -> Oslo -> Karlstad	17:00	19:00	Plane 1
Karlstad -> Gothenburg -> Karlstad	17:30	19:30	Plane 2

Table 3: Flight schedule with assigned planes

While one charger could potentially cover all the charging for both planes while still being able to keep to the flight schedule, having multiple chargers has the following advantages:

- Increased capability to add more planes in the future.
- Multiple chargers allow the charging to be distributed which decreases the stresses related to repeated heavy loads on the same line.
- It increases the reliability of the charging operation and allows for repair or maintenance of a charger without completely stalling the flights.

The downsides of incorporating more chargers are:

- Increased cost in both purchase, installation, and maintenance.
- Increases the periodic load on the system.

With this analysis two chargers in the system should be adequate to fulfill the needs while still providing a safety margin for possible faults, rescheduling or other.

Due to the limited information about the ES-19 charger, it is unclear whether the charger could charge the plane at lower power level, this would be advantageous since battery lifetime is negatively affected by higher charge rates. Having a lower power rating also has the advantage of decreasing the stress on both the chargers and on the transmission cables in the system. In this situation, it would be more advantageous to charge the planes during a period of multiple hours instead of the optimal charging time of 40 minutes.

Looking at the flight schedule plane 1 and plane 2 have a period of 9 hours between the next departure which could be used to charge the plane. The recommended charging time would be around 8 hours which would give an hour to prepare for the departure or any temporary changes to the flight schedule.

If a charging would take 40 minutes on a 1MW power level:

$$E_{FBattery} = h * P_{charger} = \frac{2}{3} * 1000\text{kWh} \tag{24}$$

$$P_{charger} = \frac{E_{FBattery}}{h} \tag{25}$$

Where $E_{FBattery}$ is the energy required to fully charge the battery from an uncharged battery, h is the hours required for charging and $P_{charger}$ is the power delivered to the charger.

Using a charge time of 8 hours:

$$P_{charger} = \frac{1000}{8} * \frac{2}{3} \approx 83{,}33kW$$

Comparing the two power modes and their daily energy consumptions:

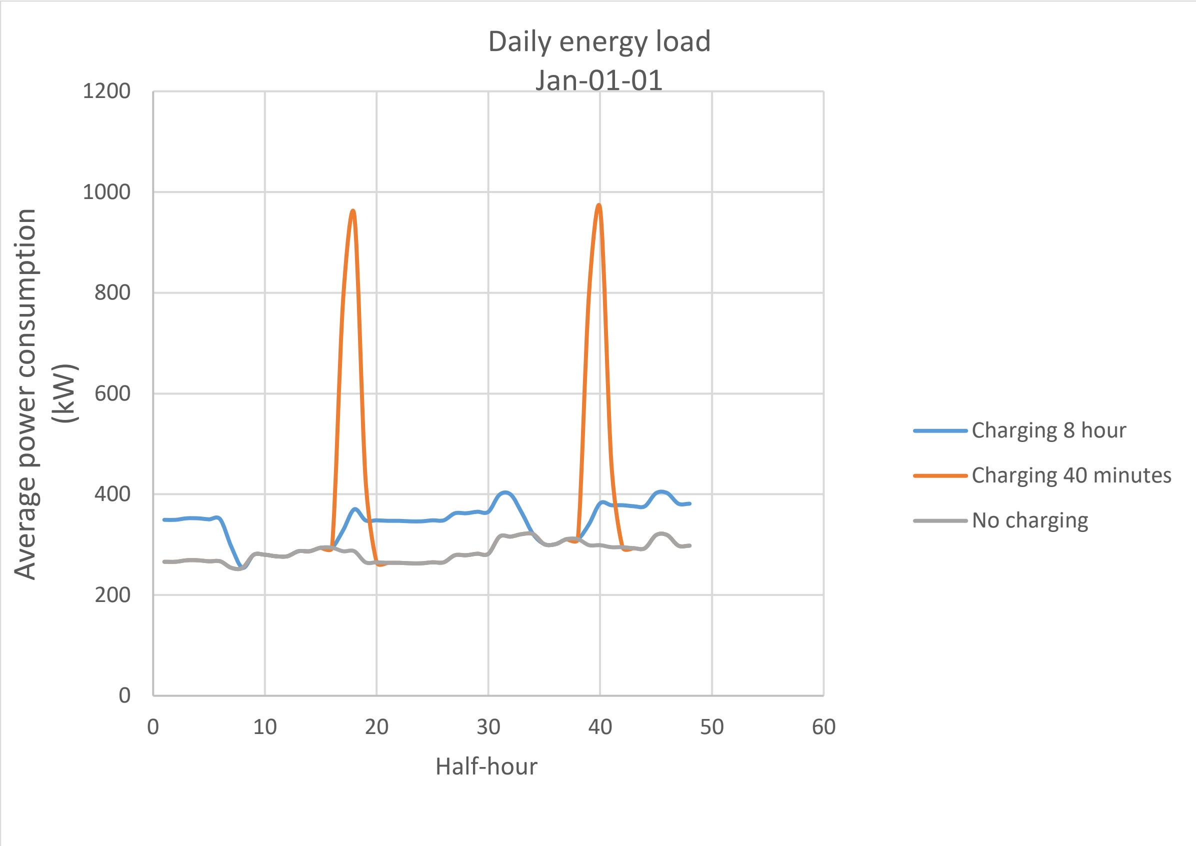

Figure 8: Average half-hour power consumption of facility. Grey curve shows the facility consumption without chanrging, blue curve shows power consumption with charging over 8 hours and orange curve shows power consumption with charging over 40 minutes.

Looking at the graph, the shorter loading time will have a much greater impact on the system during its loading time than the longer charging time. It would be highly advised to try to extend the loading time of the charging to avoid unnecessary stress on both the chargers and the grid.

4.3 Facility grid construction:

4.4 Required size for solar park:

The following calculation are under the assumption that multiple parts of the systems are static and does not change with time, not only does the solar irradiance and weather change radically from year to year, but the solar plant will degrade with time leading to decreased yearly performance. NREL studies has shown that a typical degradation speed is around 0.5% per year leading to a loss of around 10% after 20 year. [17] Since one of the goals of the project is to be able to supply green energy to the facility year around the 10% loss will be compensated by dividing the required area by a factor of 0,9. Additionally, to increase the reliability to be able to supply the facility oversizing the facility could also help to ensure that the facility has a large generating capacity even under non-ideal circumstances. To ensure the ability to provide annual energy in this project the solar modular area will be oversized to around 15% extra to have a safety margin.

By referencing Table 1 and equation (15) using the value from the most energy intense year 2019 with an annual energy consumption of 2.214GWh as E_{an}, the value 846.174 [kWh/m^2*year] from the code as G_{AN} and using efficiency values of the Power Electronics: FS3150M power inverter of around 97.011%, and efficiency of around 20.052% for the polycrystalline solar panel CSI Solar co. Ltd. CS3Y-470P. the following equation can be made:

$$A_{MReq} = \frac{2\,214\,072 * 1.15}{846.173845 * 0.2052 * 0.97011 * 0.9} \approx 16800m^2$$

The modular area required to provide the facility with solar energy would be around 1,68 hectar.

With the addition of electrical airplanes, the annual energy requirement would increase to around 2,65GWh, This would be an energy increase of around 19% which would mean that to cover the additional energy requirement the solar plants modular area would need to be 19% larger, which amounts to around 20000m^2 or around 2 hectar.

4.4.1 Simulation of the PV systems:

The system specification are selected as the following:

	Cover existing facility	**Cover facility and additional chargers**
Annual energy production [GWh] (Year 1)	2.596	3.181
Nameplate DC capacity [kW]	3,440.517	4,151.181
Total AC capacity [kW]	3,017.848	3,662.494
Inverter DC capacity [kW]	3,094.750	3,764.490
Solar cell	CSI Solar co. Ltd. CS3Y-470P	CSI Solar co. Ltd. CS3Y-470P
Inverter	Power Electronics: FS3001M [34000V]	POWER ELECTRONICS: FP3510M2
Number of solar cells	7,320	8,832
Modular Area [m^{2}]	16 762	20 225
GCR	0.5	0.5
Total Area	33524	40450

Table 4: Table over the specifications of two solar power plants suggestions.

As seen in Table 4 both systems are oversized to the inverter rating. The reason for this is that oversized systems have a higher safety margin meaning that this system can deliver power even in less ideal circumstance. The other reason is that oversizing also reduces the mismatch power loss.

The choice of having a fixed solar panel installation is based on safety because of glare. While tracking solar panels have a higher energy output than a fixed installation having tracked solar panels located around the airstrip increases the risk of glare occurring to the pilots when they come in to land the airplanes.

4.5 Storage potential through excess energy generation:

By comparing the hourly energy generation by the solar power plant with the hourly energy consumption of the facility the excess energy can be expressed as a potential storage which can be used for future charging, load shifting or selling to the grid at a more opportune time.

Comparing the power production of the solar farm with the consumption during the year 2018:

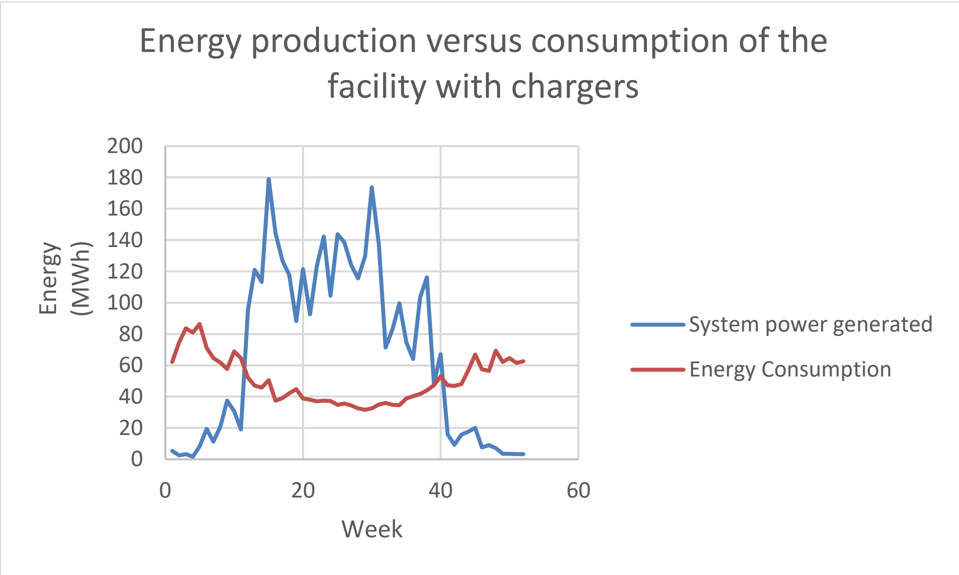

Figure 9: Weekly energy consumption of the facility versus the solar power plant production.

This shows that an excess of energy is produced during the summer and an energy deficiency occurs during the darker parts of the year. During the colder months to accommodate the increased energy consumption and reduced production a total of 1233,86MWh of energy needs to be imported from the grid even when supported by the PV production. During the summer an excess of 1783,91MWh of energy is produced. This leaves an excess of 550,8MWh of energy which could either be stored or exported directly to the grid.

Figure 9 also shows that the energy consumption of the facility exceeds the available energy production during the colder months. This shows that if the requirement of having a green airport where the energy used in the airport is 100% green, storing an excess of 1233,86MWh of energy and using that during the colder months is required.

4.6 Current grid structure:

The one-line diagram that will be constructed in this project will not be an exact copy of the diagram provided by the airport as they request that the layout not be shown in its entirety. This means that in this project the one-line diagram used here will be functionally identical, but the layout of the load, transformers and buses will not be pictorially accurate to the original diagrams provided by the airport.

The following figure shows how the functional grid looks:

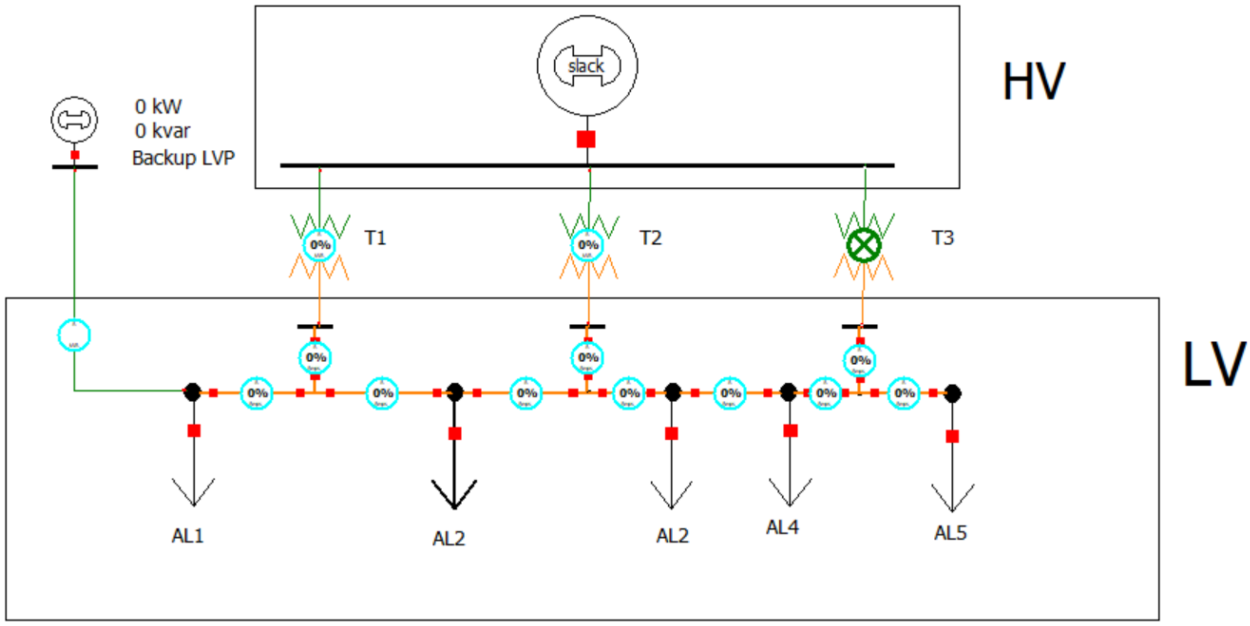

Figure 10: Functional representation of the airports one line diagram.

The grid is represented as a slack generator on the HV side, T1, T2 and T3 are the installed power transformers, each of them have a power rating of 1600kVA, AL are multiple loads aggregated into an aggregated load and the generator at Backup LVP are the generators installed in the facility that are used during LVP. T1 and T2 are the primary power transformers in the system while T3 is exclusively used during the LVP protocol.

4.7 Power through the current grid:

Inspecting the load profiles over the facility in Figure 7, it shows that the heaviest load periods occur between the months of November and February. This general trend occurs because during the colder periods of the year the systems that rely on electricity for heating are used more frequently. Because a measured continuous load over the facility is not available, estimating the load profile from the energy profile of the facility is necessary using the theory in 3.4 with the energy graph between 2017-2022.

Because the colder seasons experience a significantly higher peak energy loading these periods will be the ones that are investigated for the current status of the grid. By using the highest hourly energy consumption that occur each day between November and February from 2017 to 2022 coupled with the delivered VArh for that particular hour a peak power graph can be made:

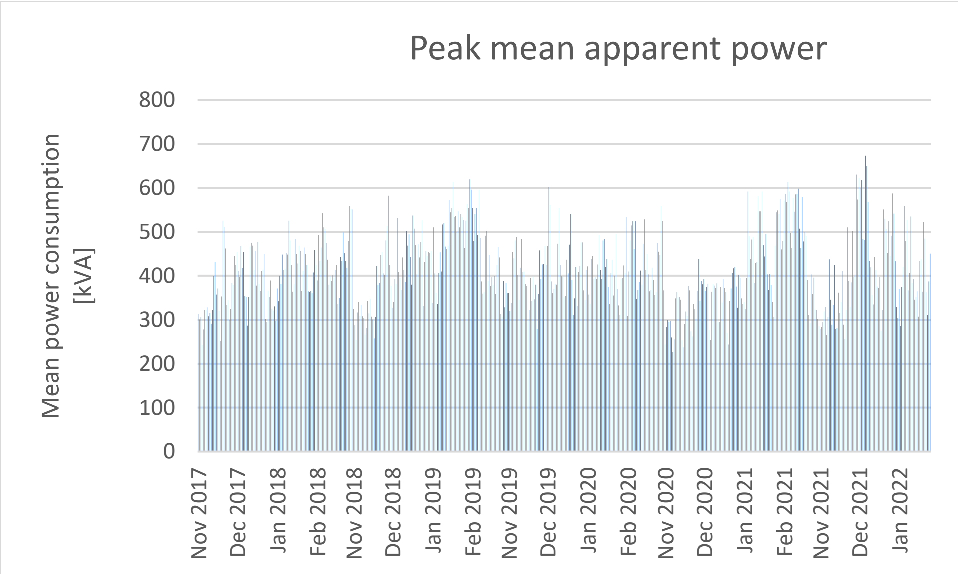

Figure 11: This graph shows the peak mean power consumption during the colder months between november and febuary.

Here the highest recorded average power consumption occurred in Dec 2021 with a value of approximately 674kVA.

As mentioned in the assumptions, because of the lack of information about either the energy or power flow through the system all of the load points in the system will be treated as equally loaded.

During the peak loading period if the assumption is that a 674KVA loading during this period the system would look like this:

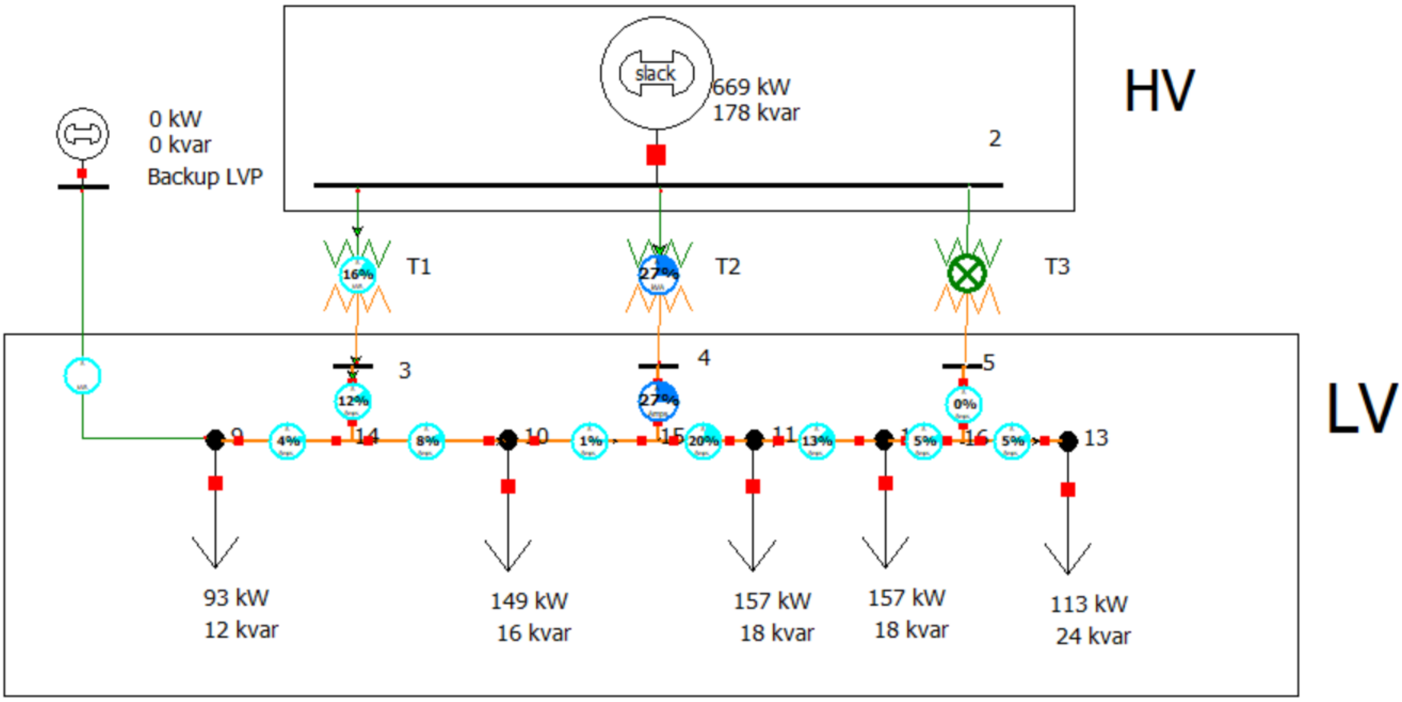

Figure 12: One line diagram of the airports grid without any additional chargers

Each of the transformers have a power rating of 1600kVA and all the connections between the nodes have a current rating of 3200A.

The LV system runs on a 400V line to line RMS voltage then the equation becomes the following:

$$\sqrt{(3)} * 400 * 3200 \approx 2216kVA$$

This means that the cables have a power rating of 2216kVA in the LV system.

While the parts of this system can survive and function even when they are overloaded over a shorter time period having the system heavily loaded over a longer period of time is unwise as this decreases the lifetime of the transmission lines and transformers in the system. In this project a power level of above 80% of the rated power is too heavy as it would dramatically decrease the service time of the transformers. [18]

This means that the rating for the transformers and cables would decrease by 20% to be an acceptable power load. This would mean that each of the transformers would have an acceptable rating of 1280 kVA and the cables have a rating of 1773 kVA.

The total load that the transformers can handle would be 2560kVA and the average apparent power load during the heaviest period is 674kVA. That would mean that the system would have 1886kVA of extra power that could be added into the system.

4.7.1 Addition of chargers into the system.

As mentioned previously in 4.2.1 the number of chargers necessary to cover the future operation would be two chargers. Additionally, it would be recommended to extend to a longer charging duration with a lower power rating to lessen the stress on the system. In Figure 12 T1 is loaded to around 16% of its rated power level while T2 is loaded to 26% of its rating meaning that if the chargers where set to the extended load setting each charger would contribute an additional 83,33kW to the system. Which would mean that two additional chargers would add a total of 167kW to the system while in the extended load time condition. Because T1 is the least loaded transformer the chargers are inserted as close to T1 as possible. The additional loads would change Figure 12 to the following:

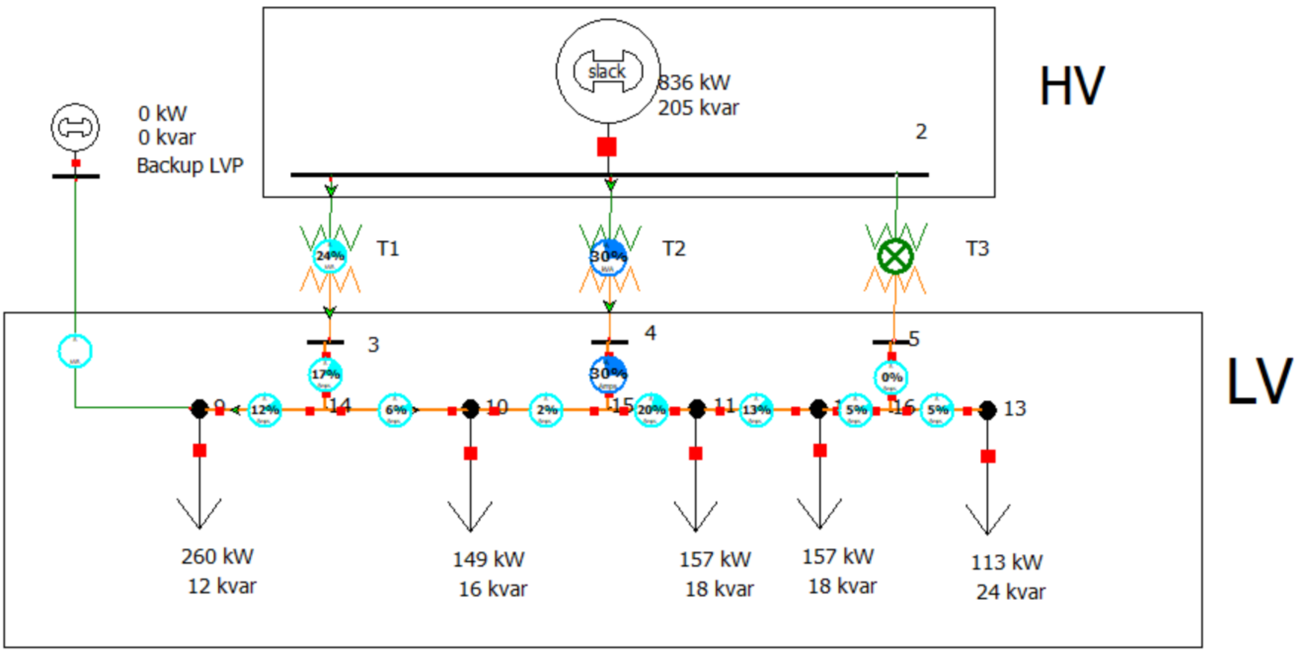

Figure 13: One-line diagram of the airport with the addition of two chargers. Each of the chargers contribute 83,33kW each

Figure 13 shows that adding the chargers to the system under the condition that the chargers would stay on a lower power rating would be feasible with no risk of overloading either the transformers or the transmission lines. While the system can handle the lower power level it is important to look at how the system would react if the charging mode of the chargers were to switch to the highest power setting. This scenario could occur either accidentally or deliberately during an unexpected change in the flight schedule or similar, the system would need to be able to handle a sudden increase in required power. Each of the chargers have a claimed charge power rating of 1MW, this would mean that a total of 2MW would need to be able to be inserted into the system. Because of the large load that each of these chargers provide, the placement of chargers will be on each end of the one-line diagram. This is to try to spread out the chargers' impact on each of the transformers. Inserting the chargers into the system gives the following one-line diagram:

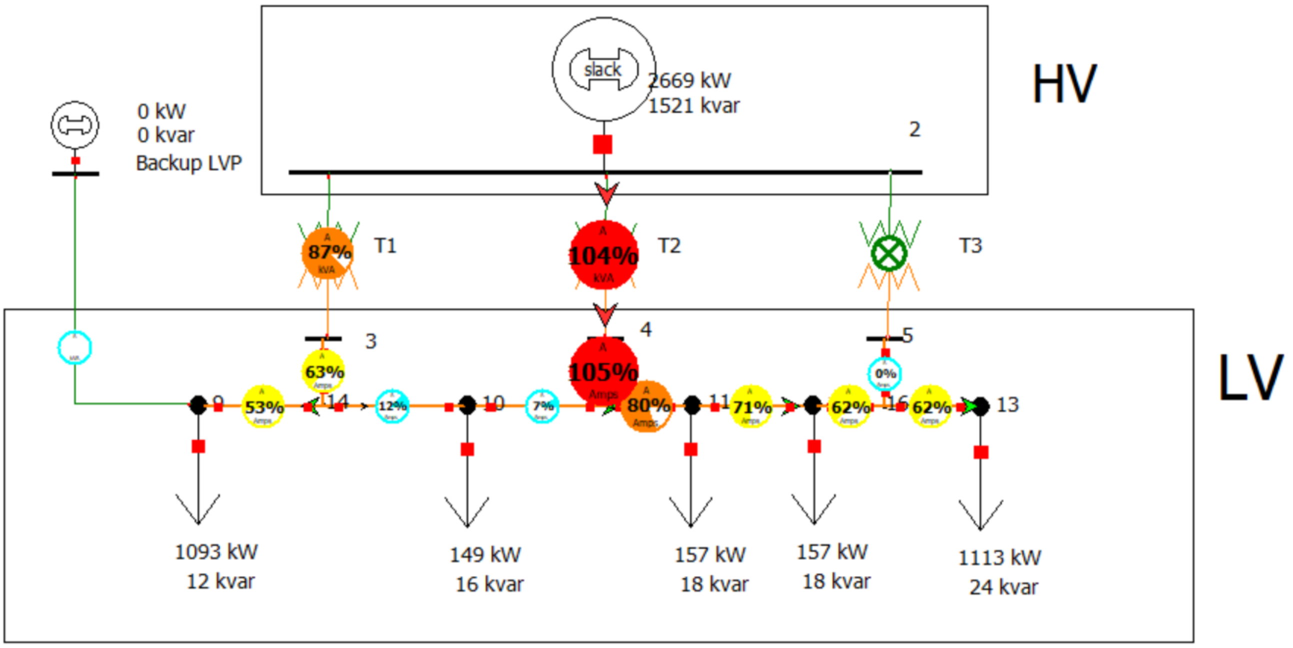

Figure 14: One-line diagram with additional chargers. Charger 1 is placed on bus 9 and charger 2 on bus 13. Each of the chargers here consume 1MW.

Figure 14 show that inserting the chargers directly to the system could potentially overload the power transformers in the system.

4.8 Embedding LVP into the system:

LVP is a protocol that comes in effect when visibility is limited around the airport. The goal of the LVP is to ensure that the necessary equipment can be supplied by a reliable energy source for a duration of up to two hours. At this moment the airports LVP system consists of three diesel generators able to supply the airstrip for a duration of up to at least two hours. When LVP activates, the system disconnects T1 and islands parts of the system to ensure that the crucial parts of the airport are energized. T3 is closed to support T2 for the entire duration of the LVP. During LVP the system looks like the following:

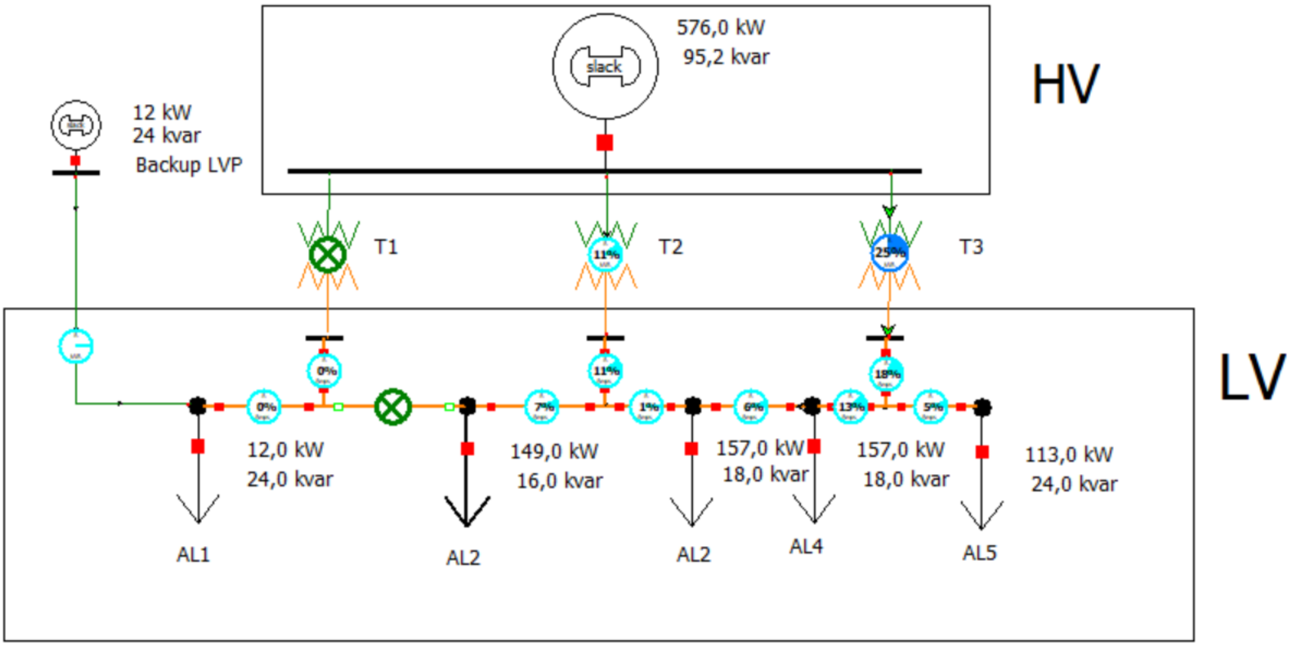

Figure 15: One-line diagram of the system during LVP.

During LVP AL1 needs to be supplied for a minimum of two hours. Because the LVP disconnects all other loads and keeps the designated equipment on constantly during LVP AL1 can be seen as a constant load. Because the load is constant under a duration of two hours that would mean that an energy storage of at least 24kWh would be necessary to supply the designated equipment.

4.9 Connecting PV system into the grid:

Assuming the placement of the PV plant would happen as close to the airport as possible a suggested placement would be the following:

Figure 16: Sattelite picture of the airport. The blue outline shows the size that the suggested solar power plant would occupy.

This area is suggested because the solar panels are not directly next to the airstrip which might interfere with the safety for incoming flights**.** The rough distance cable required to connect this into the grid is show below:

Figure 17: Sattelite picture of the facilities around the airport. The white lines are the suggested pathway for the transmission cables between facility and solar production.

This path does not cross any airstrips which could potentially shut down parts of the operation during installation. As shown in Figure 17 the cable required would need to be roughly 600m. The cable required would be something like a 33 kV 3x70 XLPE cable.

Because the transmission line has a phase-to-phase voltage of 34,5kV a power transformer would be necessary to connect the transmission line to the LV grid. This would require a transformer with a turn ratio of 86,25. Because the grid cables have a rated power of 2217kVA and the total power generated from the PV plant is around 3,5MW connecting the PV plant directly into the LV line would overload the cables. This is under the assumption that all the excess power that is not used will be exported to the mains through the LV network. A solution would be to connect the LV line for use in the LV system and designate a new power transformer to export the excess power to the mains.

5. Discussions:

5.1 Evaluating possible placements of the future solar plant:

Placement of the solar power plant impact the efficiency, cost and complexity of the network since it influences the distance that the power has to travel for delivery to the consumption point. In general placement of any generator should be as close to the consumption as possible to reduce losses in transmissions.

This project faces difficulties about the placement of the ESS and solar power plant due to the fear of EMI to the airspace communication devices on the premise of the airport. This concern come from a statement made by LFV where facilities with the risk of producing EMI would need to be situated a distance away from the airport. LFV have strongly recommended any solar installation to be situated 3km away from the airstrip. [19]. According to the airport the strong recommendation by LFV can be argued against by the client but they would need to prove that no significant EMI could occur from the facility which would mean that the facility would have to be constructed to be assessed. Situating the solar power plant 3km away would require extra implementations such as:

- A 3km long cable to connect both the solar park and the airport
- Purchasing or leasing land for the construction of the solar park and acquiring the land necessary to connect both facilities.
- An extra high-power transformer specifically to take down the high transmission voltage down to the lower voltage levels**.**

The line voltage drop can be expressed as:

$$\frac{S_{3p}}{V_{LL} * \sqrt{3}} * L * \sqrt{R^2 + X^2} = \Delta V_{LN} \quad (26)$$

Where S_{3p} is the total power transmitted through the cable, V_{LL} is the line-to-line voltage, L is the length of the cable in kilometres, R is the maximum AC resistivity of the cable per kilometre, X is the maximum reactance of the cable per kilometre and ΔV_{LN} Is the single phase voltage drop in the cable**.**

Using data about the 33 kV 3x70 XLPE cable gives the following values comes out [20]:

$$3.5 * \frac{10^6}{34{,}5 * 10^3 * \sqrt{(3)}} * 3 * \sqrt{0.06^2 + 0.101^2} \approx 21V$$

This would mean that a 21V line voltage drop would equate to a phase-to-phase voltage drop of around 36,4V. Using Elsäkerhetsverkets regulation about voltage differences its stated that a voltage difference between ±5 nominal voltage is accepted, a 36,4V difference on a 34,5kV would be approximately a 0.11% voltage difference which is acceptable. The electrical losses due to the additional cable would be:

$$P_{3\Phi\text{loss}} = 3 * P_L = 3 * Z_{cable} * I_L^2 \tag{27}$$

$$I_L = \frac{P_{3\Phi}}{\sqrt{3} * V_{LL}} \tag{28}$$

$$I_L = \frac{3{,}5 * 10^6}{\sqrt{3} * 34{,}5 * 10^3} \approx 58{,}571\ A$$

$$3 * 58{,}571^2 * \sqrt{0.06^2 + 0.101^2} \approx 1209W$$

This would be a miniscule power loss when comparing the power transmitted which is around 3.5MW.

While a 3km transmission line would be feasible it would increase the cost of the project due to the increased cost of additional land and equipment. The recommended placement of the solar plant would as close to the facility as is feasible because of the following reasons:

- The area around the airport is owned by the airport itself which then requires no extra steps to own the land.
- The area around the airport is already flattened which reduces the work necessary to level the ground to be used in the solar plant which reduced the cost.
- Reduces the work and cost required for installing the transmission lines.
- Increases the ease of expanding the solar power plant for future load needs.

5.2 Evaluating the daily load peaks:

Inspecting Figure 11 it shows no significant trend over time. Since no significant increase in the load has occurred over the last five years this project will not focus on estimating the future load profile of the airport. This project will focus on the impact of adding the chargers to the system.

5.3 SAM:

SAM is a simulation tool developed by NREL for use in modelling future renewable energy production and storage. This system has access to modelling for a variety of renewable energy and storage systems such as photovoltaics, wind power, battery ESS and fuel cells. [21] SAM allows for a variety of sizes of the systems ranging from small rooftop installations used for residential load supplying to large scale power generation and storage used for power quality and load shifting.

SAM allows for both evaluation on the economical as well as the technical parts about the future system using the specification of the future system provided by the user.

The information provided through the simulation includes general information about the systems performance and cost, this includes the annual energy production, the systems capacity factor, energy yield, total cost, etc.

SAM allows for different commercial models including.

- Residential and commercial projects
- Power purchase agreement (PPA) projects
- Third party ownership

Alternatively, SAM allows for a modelling system where the economical aspect is absent and instead looks at the performance of the system as a power generating facility.

This project will be using the non-financial photovoltaic simulation model as this project is mainly focused on the technical requirements to be able to supply energy to the facility and not a detailed combined techno-economical study.

5.4 Future grid design:

5.4.1 Design of the PV system:

In solar power plants the arrangement of the solar panels and power inverters is called architecture. Architectures vary the connections between the solar panels and inverters and the configurations of these.

There are 4 main architecture designs when designing solar plants: [22]

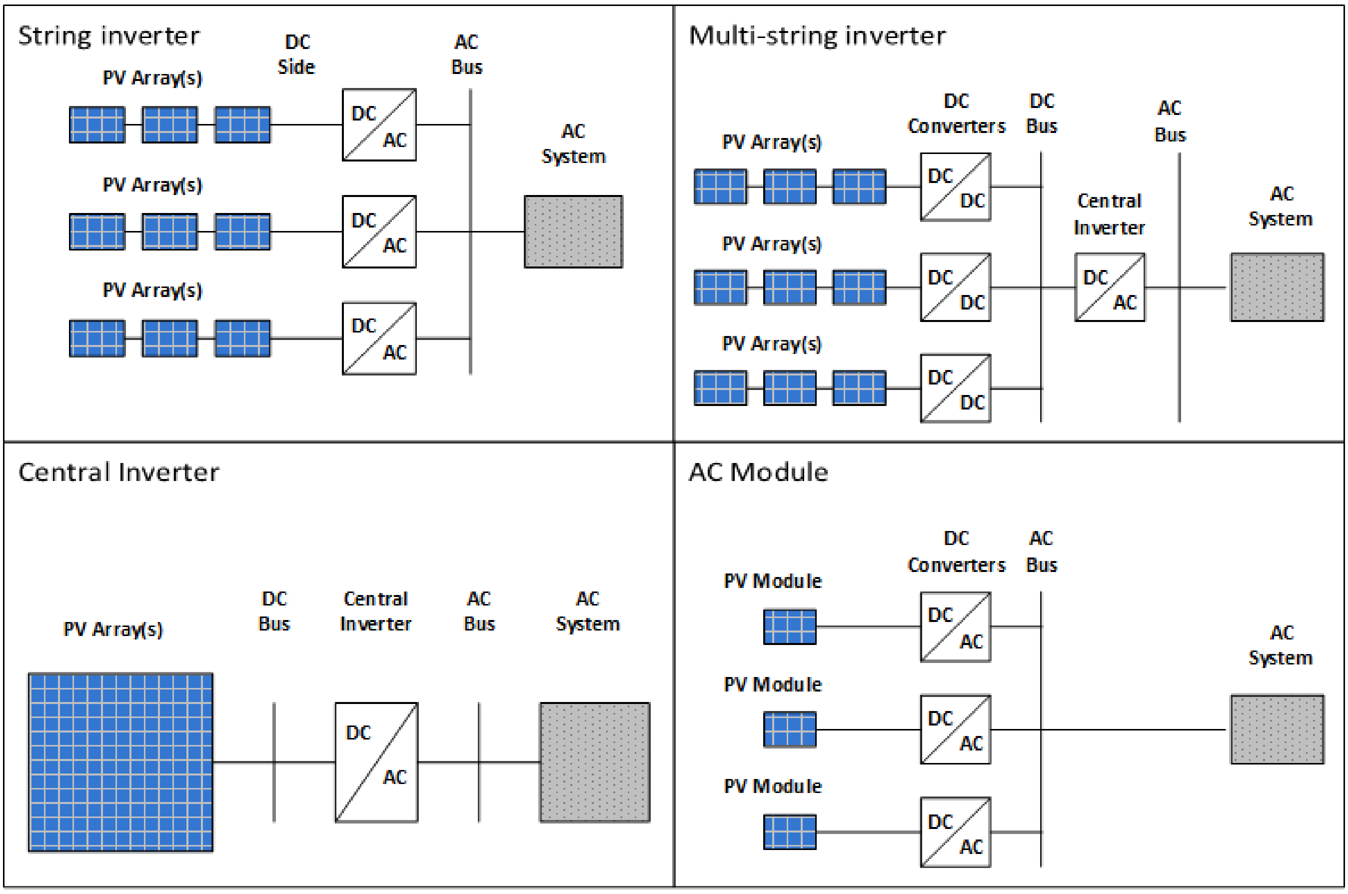

Figure 18: The four main architectures.

Central power inverter:

This configuration consists of a single central power inverter where all the strings of solar panel are connected in parallel to the central power inverter in this configuration the central power inverter function as both the MPPT and the power inverter. Because of this design only requiring one large power inverter it is a cheaper and highly efficient design being optimal for large scale power productions. The drawbacks of this type of design would be an increase in losses due to voltage mismatches between the pv strings, installation requires high voltage DC cables for connecting the solar panels and inverters and a loss of reliability because all power production goes through a single inverter.

String:
In this configuration each string of solar panels is equipped with its own MPPT inverter. Because each string has its own MPPT this leads to low losses due to voltage mismatch between the strings, leading to high roundabout efficiencies and removing the necessity of a string diode in each string. One of the drawbacks could potentially be a higher cost because each string requires its own inverter.

AC module:
In this configuration every solar panel is equipped with a MPPT inverter that is then connected into a DC/AC converter.
This design lends itself to a high efficiency as there is no mismatch losses and each solar panel can operate at its MPP at all times, has the highest reliability since failure of any solar panel or its inverter does not disturb the production of any other panel and increased flexibility for additional solar panels because installation just requires the addition of the solar panel and its power inverter.
The highest drawback to this design is its high installation cost and losses due to high voltage boosting which makes this configuration unsuitable for large scale power applications.

Multi-string inverter:
This converter combines the design of the central inverter and string module architecture by including a MPPT inverter on each string of solar panels and guiding it into a central power inverter. This design combines the advantages of the central and string configuration leading to high efficiency and low mismatch losses. This design does increase the installation cost of the solar plants and lower reliability as in the case of the central inverter.

As mentioned in 5.1 one additional concern is the EMI emitted by inverters. This leads to decreasing the number of inverters present in the system as a priority to avoid the risk interference in the communication technology around the airport. For this project the architecture of choice will be the central inverter type because of the minimal number of inverters. If the danger of EMI were not to be considered the multi string inverter configuration would be considered because of the increased efficiency.

5.4.1.1 Required solar park:

As shown by the results from Table 4 the required solar park to annually supply the airport and future airplane chargers with solar energy would need a system with around 8,832 solar panel. This system would use the central inverter architecture having only one power inverter which all of the power was fed to. This entire solar park would occupy around 4 hectares of land and the system has the capability to deliver 3,66MW of power during optimal operation.

5.4.2 Design of the storage system:

During this project another project going alongside it investigated the most economically viable storage system required for this project [23]. In the referenced project the storage system was between either hydrogen or battery ESS. The result was that the best option for the large energy storage requirements would be to go with a hydrogen power plant because of its lower energy storage cost. However, since investigating the most appropriate ESS is outside the scope of this project the ESS presented in this project could potentially be any type of ESS.

Storage systems can be arranged in a multitude of configurations. Some of the different configurations can be the interconnectivity between the solar power plant and the ESS or if the ESS will be in a central hub or distributed out to different parts of the system. These things will quickly be discussed here to evaluate what is the best solution for this case.

Interconnectivity with power production and storage:

Storage systems can be interconnected to the power production through a DC/AC link between each of the systems inverters. This would look like the following:

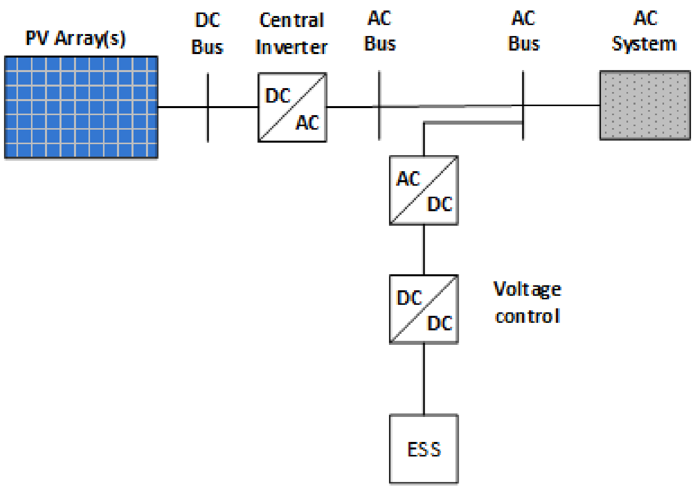

Figure 19: Seperate ESS and power production. The systems could be linked together anywhere in the AC system.

This configuration lends the ability for the two systems to be allocated at different locations and increases reliability since each of the systems works through separate inverters. The main disadvantages might be an increased cost due to the additional components required and it might decrease the roundabout efficiency of the system because of the additional component required in the system.

Another way to connect the systems together is to link the DC busses of both the power production and storage together and binding the shared DC bus to a shared inverter:

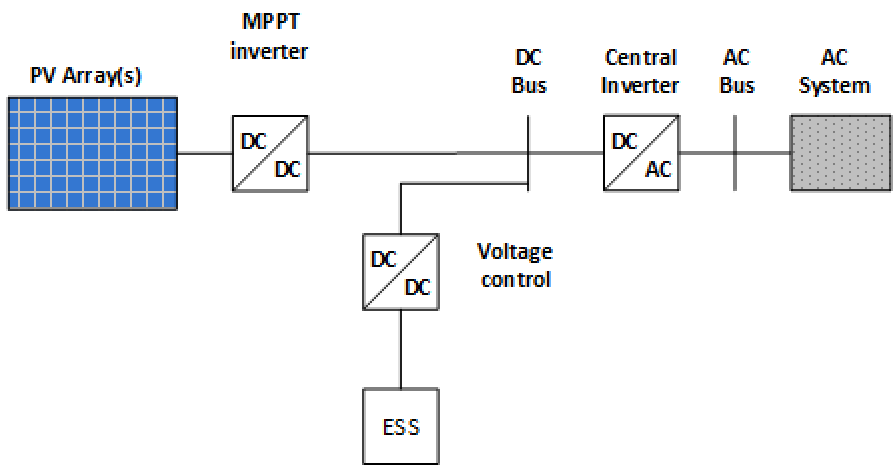

Figure 20: Power production and ESS interconnected to a shared DC bus.

This system might lend itself to a higher efficiency and a decreased component cost. But here the reliability of the system decreases because the production and storage are linked to the same power inverter. This could be offset by having multiple inverters at the same location, but this might increase the cost, maintenance and risks reducing the efficiency of the system due to the potential of having the inverter operate at a low power loading which in turn reduces its efficiency.

Centralized or distributed systems:

The energy storage system can either be located at a central hub or distributed through the system. Each of these would have a different impact on the system and different advantages and disadvantages.

A centralized system would mean that independent of how the system is interconnected with a power production most of the stored energy would occur in one central hub. This system has the advantage that because less component is required the need for extra equipment or maintenance decreases which in turn makes this a more economical option. But this has an impact on the reliability of the system since a failure in one of the components could lead to a complete shutdown of normal operation.

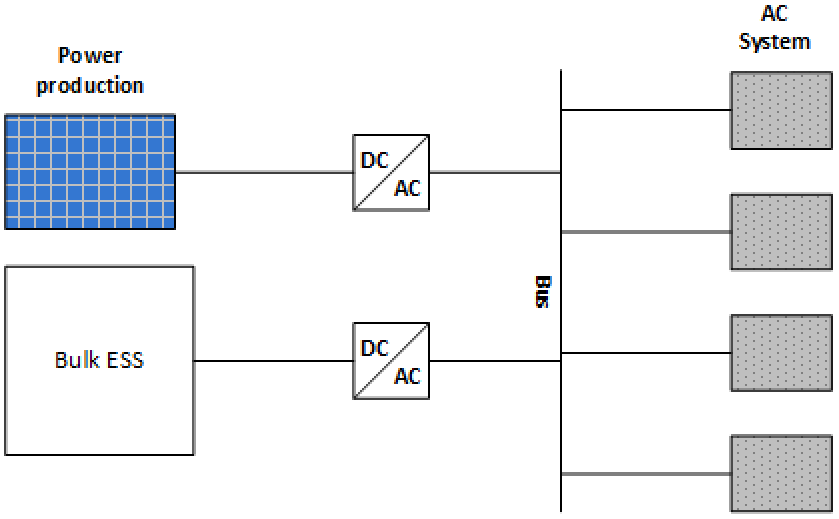

Figure 21: A single central ESS that supplies all parts of the AC system.

A decentralized system would mean that the energy storage systems are not centralize to one location but spread out to several locations. This could mean that multiple smaller energy systems are distributed to important loads while the bulk of the energy storage could still be located at a larger energy system somewhere else. This system has higher reliability that depends on the amount of distributed ESS since failure of a single ESS would not completely stop any other ESS. The drawback of this system might be an increased cost and maintenance required to keep the system operating.

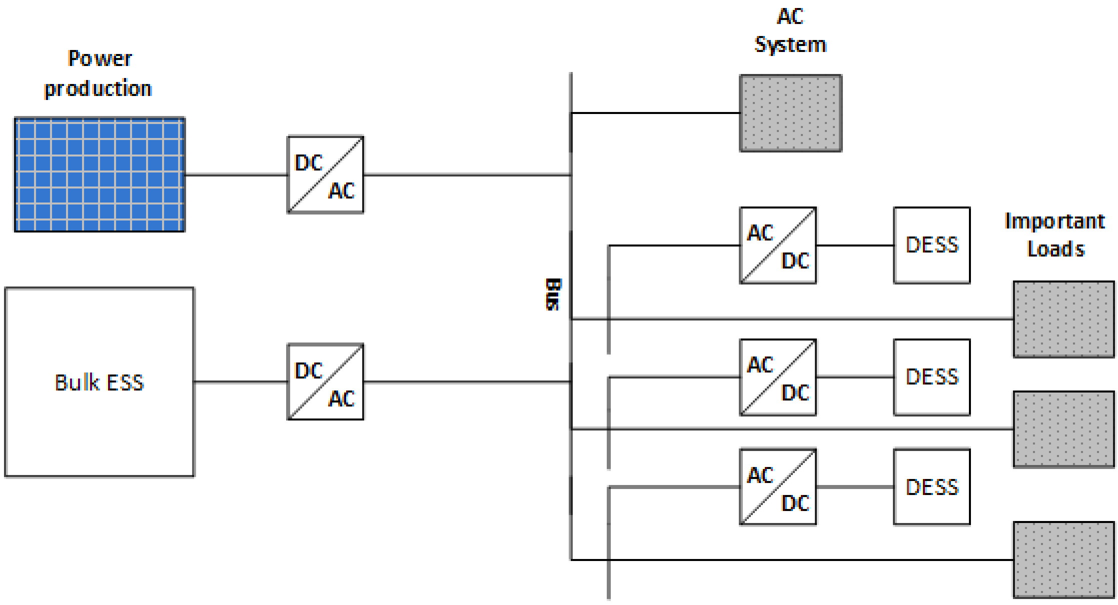

Figure 22: Multiple ESS exists. In this configuration the DESS supply important loads during high power demand periods.

5.4.3 Storage system:

As seen in Figure 9 the solar power plant would not be able to supply the facility year around with green energy. During the colder months the solar plant cannot supply the airport and the future chargers alone but requires an energy storage system that can store and supply a total of 1233,86MWh during the colder months to compensate for the production deficit. Also, to be able to accommodate the highest power peak in the current system and the addition of chargers at the optimal power setting, the storage system would need to be able to supply at least 2669 kW of power. For this system the energy storage system will consist of a central storage hub where the majority of the energy is stored during the year while each of the chargers additionally will have their own distributed ESS.

5.5 Microgrid or conventional interconnection with the current grid

Conventional:

Connecting it conventionally would mean that connecting the new system as it were a part of the original grid. This has the advantages of generally lower cost as no additional equipment except for the converters or transformers that are necessary to connect these two points together.

Microgrid:

Micro grids are defined as a group of interconnected loads and distributed energy resources within clearly defined electrical boundaries that acts as a single controllable entity with respect to the grid.

A microgrid can connect and disconnect from the grid to enable it to operate in both grid-connected or island-mode [24]. This could effectively reduce the carbon emissions from both the primary consumer but also lend to reduce the carbon footprint of a secondary consumer as well. The idea of microgrid use for renewable energy resources have in recent times become a popular suggestion for both increasing the efficiency of the renewable energy reserve but also in use to assist the local electrical grid with power during peak load hours. This could potentially help to stabilize power quality with the help of local load shifting and use in voltage regulation. If this system incorporates energy storage systems as well the grid owner could request a certain amount of energy for the highest peaks thus leading to decreased stress in the power grid. This implementation would increase the construction costs but could overall increase profits because of increased control over when to export energy into the mains.

Because of this project aim to implement its own energy generation and storage this system could benefit form integrating microgrid infrastructure and technology.

5.6 Future system:

In this system the PV system and the ESS would be interconnected to each other via a DC network to decrease the number of conversions in between generation and storage which could potentially increase the efficiency. The ESS would be a distributed ESS where one larger central hub would store energy to supply the LV AC system while the chargers would be supplied by their own distributed ESS.

The chargers would be connected into the new DC network while the existing AC LV will be bridged with a DC/AC converter.

Excess power generation would be exported through a designated power inverter interconnecting the DC side with the HV grid.

Combining the points made in the sections above into a proposed system would yield the following system:

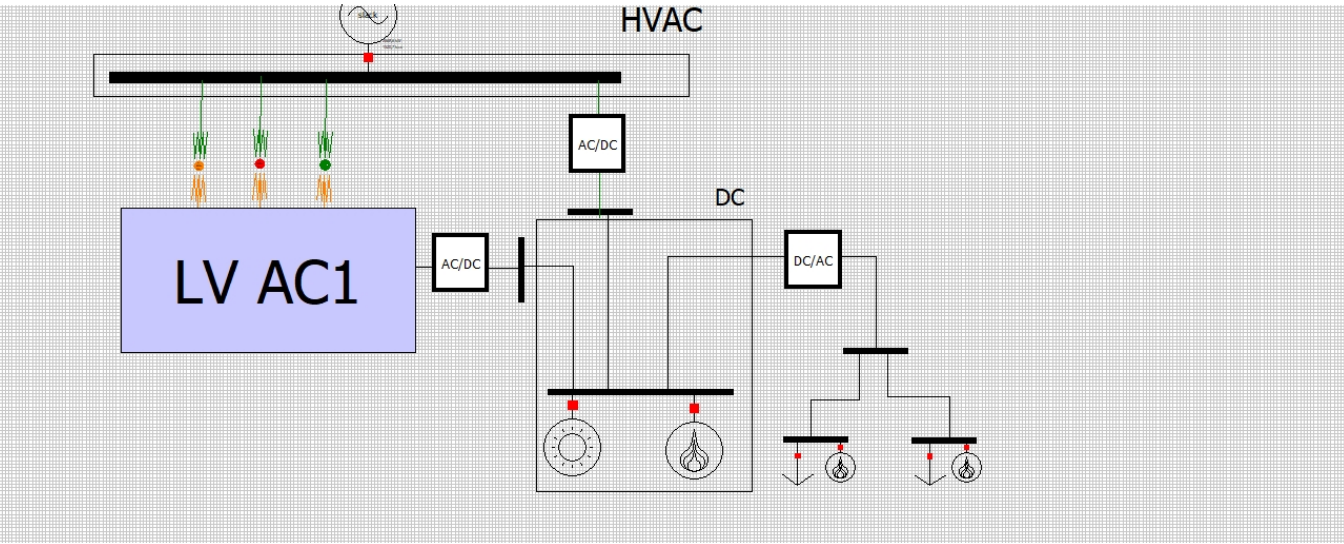

Figure 23: The one line diagram of the future system. The generator with a sun is the power production while the generator with a flame is a storage system.

The main reasons for choosing these aspects are as follows:

- Central inverter because of the decreased risk of EMI as required by LFV to follow recommendation and not risk the PV system being deemed an EMI hazard.
- Storage system and power generation interconnected to increase the efficiency between energy production and storage.
- The storage system will consist of a main large storage hub where the majority of energy storage will occur but may have additional ESS at important loads. The important loads consist of the chargers and to be able to supply the current LVP with energy for at least two hours.
- The entire new part of the grid will be a separate microgrid where the power production, storage and additional loads will be in this microgrid. The main advantages might be an increased efficiency between the energy production and storage as there are less conversions. Also having the system as a separate microgrid makes it easier to expand the system in the future since it does not require all operations to seize during the expansion.

6. Conclusion:

The main objective of this project was to investigate, evaluate and propose a possible implementation of a future green airport. This project proposes using a pv system having a total of 8,832 CSI Solar co. Ltd. CS3Y-470P solar modules arranged in a central inverter architecture as this design when simulated can supply both the current facility and also able to supply the addition of chargers into the system. Investigations of the current load profile of Karlstad airport using the energy consumption profile, analysing specifications about the current system and overlaying the additional consumption from the chargers into the airports current load profile led to the conclusion that inserting the chargers directly into the system with no modification would pose to great of a risk at overloading the current facility. Additionally, this project investigated possible configurations of the future system and lastly proposed a new future grid capable of producing and delivering the power necessary to support the chargers and the current existing facility with the help of an ESS. While this project has provided a suggested implementation the avenue of green airports needs to be investigated to fully explore its potential as future green solution. To fully explore the project like the one proposed a complete techno-economical study would be required to explore the economic and technical implications for a system like the one proposed, additionally because green airports could become significant energy producing facilities studies about the power quality in a microgrid like the one suggested in this project could be important because of their potential roles as power quality regulation centers and large energy storage hubs. Lastly because of the large amount of energy produced and exported in these types of facilities coupled with the suggestion of implementing a microgrid into this future facility studies focusing on smart grid and smart energy market management systems incorporated into similar facilities as these technologies could in the future help in power quality management and more efficient power exporting algorithms.

7. Appendix:

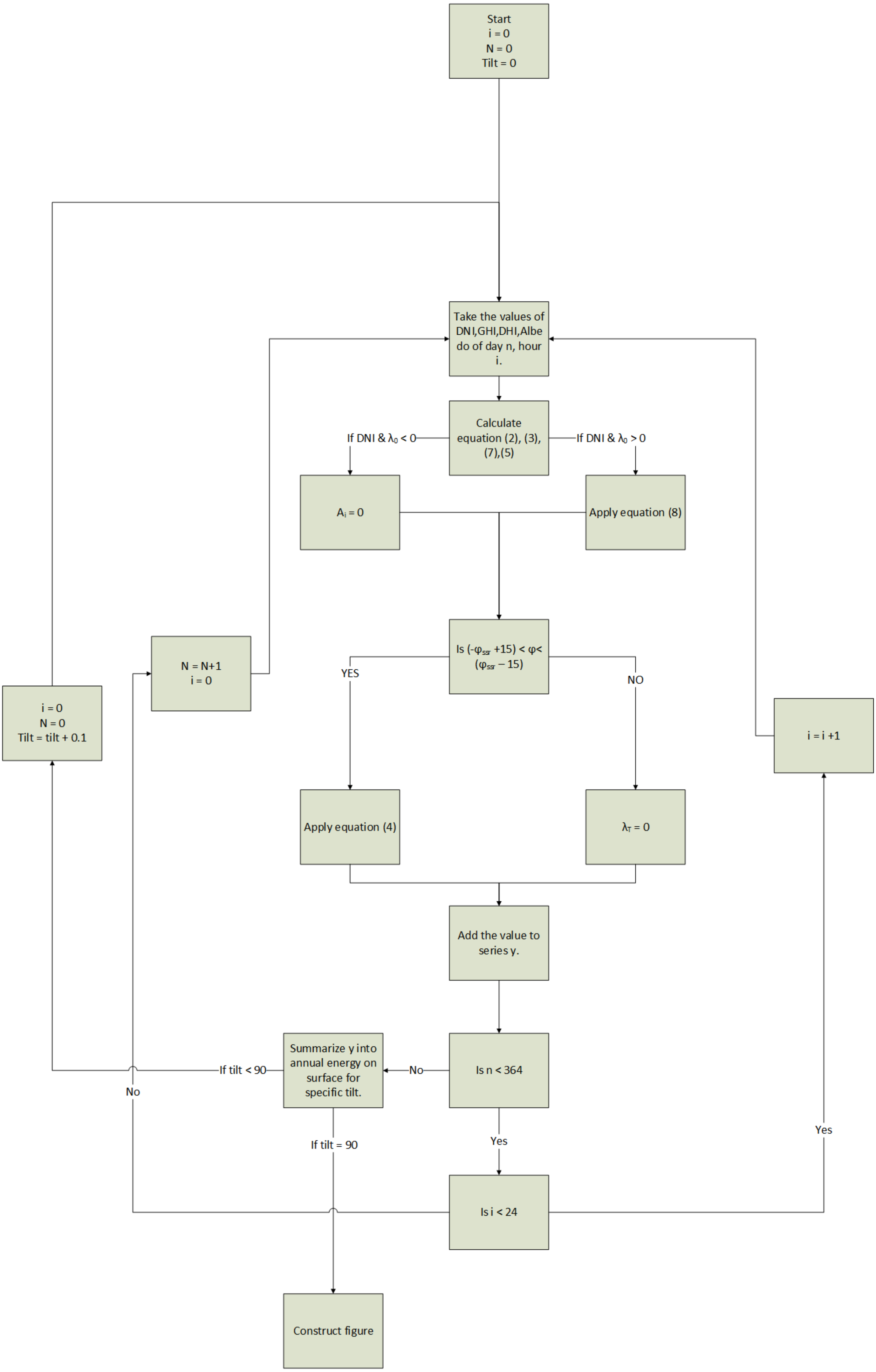

Start
i = 0
N = 0
Tilt = 0
Take the values of DNI,GHI,DHI,Albedo of day n, hour i.
Calculate equation (2), (3), (7),(5)
If DNI & λ0 < 0
If DNI & λ0 > 0
Ai = 0
Apply equation (8)
Is (-φssr +15) < φ< (φssr – 15)
YES
NO
N = N+1
i = 0
i = 0
N = 0
Tilt = tilt + 0.1
i = i +1
Apply equation (4)
λT = 0
Add the value to series y.
Summarize y into annual energy on surface for specific tilt.
If tilt < 90
No
Is n < 364
No
If tilt = 90
Yes
Yes
Is i < 24
Construct figure

Figure 24: Code Flowchart. This code is what generates Figure 6.

8. References

[1] "Statista," Karlstad University, 12 April 2022. [Online]. Available: https://www.statista.com/statistics/564769/airline-industry-number-of-flights/. [Accessed 27 May 2022].

[2] S. Johansson, J. Persson, S. Lazarou and A. Theocharis, "Investigation of the Impact of Large-Scale Integration of Electric Vehicles for a Swedish Distribution Network," *Energies*, p. 12, 2019.

[3] H. Maninnerby, S. Bergerland, S. Lazarou and A. Theocharis, "Electric Vehicle Penetration in Distribution Network: A Swedish Case Study," *Applied system innovation,* no. 2, p. 19, 2019.

[4] A. Theocharis, A. Tzinevrakis, V. Charalampakos, J. Milias-Argitis and T. Zacharias, "Transformer modeling based on incremental reluctances," in *2010 International Conference on Power System Technology*, Zhejiang, 2010.

[5] A. D. Theocharis, J. Milias-Argitis and T. Zacharias, "A systematic method for the development of a three-phase transformer non-linear model," *International Journal of Circuit Theory and Applications,* vol. 38, no. 8, pp. 797-827, 2010.

[6] H. H. Alhelou and M. Golshan, "Chapter 11 - Decision-making-based optimal generation-side secondary-reserve scheduling and optimal LFC in deregulated interconnected power system," in *Decision Making Applications in Modern Power Systems,* Academic Press, 2020, pp. 269-299.

[7] T. Andreas, M. Popov and V. Terzija, "Computation of internal voltage distribution in transformer windings by utilizing a voltage distribution factor," *Electric Power Systems Research,* vol. 138, pp. 11-17, 2016.

[8] A. Theocharis and E. Pyrgioti, "Development of a linearized photovoltaic generator model for simulation studies with electromagnetic transient programs," *International Transactions on Electrical Energy Systems,* vol. 25, pp. 454-470, 2014.

[9] P. Aupke, A. Kassler, A. Theocharis, M. Nilsson and M. Uelschen, "Quantifying Uncertainty for Predicting Renewable Energy Time Series Data Using Machine Learning," *Engineering Proceedings,* vol. 5, no. 1, p. 50, 2021.

[10] A. D. Theocharis, V. P. Charalampakos, A. Drosopoulos and J. Milias-Argitis, "Equivalent circuit of photovoltaic generator using Newton-Raphson algorithm," *Emerald Group Publishing Limited,* vol. 31, no. 4, pp. 1224-1245, 2012.

[11] A. D. Theocharis, E. C. Pyrgioti and I. A. Naxakis, "Modelling of Photovoltaic Generators Based on a Linarized Equivalnet Circuit," in *International Conference on Renewable Energies and Power Quality*, Santiago de Compostela, 2012.

[12] A. Theocharis and S. Hamanee, "Battery Storage at the Secondary Distribution Electricity Grid Battery by Investigating End-Users Load Demand Measurements," *Energies,* vol. 15, pp. 12-14, 8 April 2022.

[13] A. Nammouchi, P. Aupke, A. Kassler, A. Theocharis, V. Raffa and M. D. Felice, "Integration of AI, IoT and Edge-Computing for Smart Microgrid Energy Management," in *2021 IEEE International Conference on Environment and Electrical Engineering and 2021 IEEE Industrial and Commercial Power Systems Europe*, Bari, 2021.

[14] O. Nyquist and P. Åberg, "SVT Nyheter," SVT, 13 August 2021. [Online]. Available: https://www.svt.se/datajournalistik/solligan-2021/. [Accessed 10 Mars 2022].

[15] W. A. Beckamn and J. A. Duffie, "Directions of Beam Radiation," in *Solar Engineering of Thermal Processes*, New Jersey, John Wiley & Sons, Inc., 2013, p. 13.

[16] "What is NSRDB," National Renewable Energy Laboratory, [Online]. Available: https://nsrdb.nrel.gov/about/what-is-the-nsrdb. [Accessed 24 11 2022].

[17] B. Mow, "STAT FAQs Part 2: Lifetime of PV Panels," National Renewable Energy Laboratory, 23 April 2018. [Online]. Available: https://www.nrel.gov/state-local-tribal/blog/posts/stat-faqs-part2-lifetime-of-pv-panels.html. [Accessed 30 September 2022].

[18] N. Chen, K. Lu, W. Zhao, L. Wang and T. Dai, "Overload Analysis of Distribution Transformers Based on Data Mining," *Conference Series: Materials Science and Engineering,* vol. 439, no. 3, p. 1, 2018.

[19] K. Fors, S. Linder and T. Ranström, "Radiostörningar från solcellsanläggningar – Kartläggning av störningsproblematik i Sverige och," Totalförsvarets forskningsinstitut (FOI), Stockholm, 2020.

[20] "APDCL," [Online]. Available: https://www.apdcl.org/website/docs/tech_spec/6.pdf. [Accessed 17 09 2022].

[21] "NREL," National Renewable Energy Laboratory, [Online]. Available: https://sam.nrel.gov/. [Accessed 01 07 2022].

[22] M. Ahmad, "Selection of Inverters for PV System," in *Operation and Control of Renewable Energy Systems*, Chichester, John Wiley & Sons, 2018, pp. 307-310.

[23] *An airports' need of change to go 100% green using an energy storage system and solar power,* Karlstad: Karlstad University, 2021.

[24] M. Ahmad, "Microgrid," in *Operation and Control of Renewable Energy Systems*, Chichester, Johm Wiley & Sons, Ltd, 2018, p. 326.